Individual Variation in Brain Network Topology and Social Cognitive Ability

Ling, George*[12], Lee, Ivy*[12]; Guimond, Synthia[12]; Lutz, Olivia[12]; Tandon, Neeraj[12]; Öngür, Dost[23]; Eack, Shaun[4]; Lewandowski, Kathryn[23]; Keshavan, Matcheri[12]; Brady Jr., Roscoe[123].

[1] Department of Psychiatry, Beth Israel Deaconess Medical Center, Boston, MA, United States.

[2] Department of Psychiatry, Harvard Medical School, Boston, MA, USA.

[3] Schizophrenia and Bipolar Disorder Program, McLean Hospital, Belmont, MA, USA.

[4] University of Pittsburgh, School of Social Work, Pittsburgh, PA, USA.

*These authors contributed equally to this manuscript

Address correspondence to:

Roscoe Brady Jr.

robrady@bidmc.harvard.edu

Funding:
This work was supported by the National Institutes of Health:
K23MH100623 (RB)
RO1MH92440 (SE, MK)
K24MH104449 (DO)
K23MH091210 (KL)

Conflicts of interest:
DO: Served on Scientific Advisory Board for Neurocrine Inc in 2016
All other authors report no conflicts of interest

This work is not peer-reviewed.

Abstract

Background: Social cognitive ability is a significant determinant of functional outcome and deficits in social cognition are a disabling symptom of psychotic disorders. The neurobiological underpinnings of social cognition are not well understood, hampering our ability to ameliorate these deficits.

Objective: Using a data-driven approach, we sought to identify the brain network basis of social cognition using a combination of fMRI (functional magnetic resonance imaging) and a validated measure of social cognition.

Methods: Study participants included 60 participants with a diagnosis of schizophrenia or schizoaffective disorder and 46 healthy comparison participants. All participants underwent a resting-state fMRI scan. Social cognition was measured using the MATRICS battery of cognitive tests. A data-driven, connectome-wide analysis of brain connectivity examined how each individual brain voxel's connectivity correlated with social cognitive performance using multivariate distance matrix regression (MDMR).

Results: We identified a region in the left superior parietal lobule (SPL) where individual network topology predicted social cognitive ability. Specifically, the association of this region with the Default Mode Network predicted higher social cognitive performance and association with the Dorsal Attention Network predicted poorer performance. This correlation was observed in both schizophrenia and healthy comparison participants.

Conclusion: Previous studies have demonstrated individual variance in brain network topology but the cognitive or behavioral relevance of these differences was undetermined. We observe that the left SPL, a region of high individual variance at the cytoarchitectonic level, also demonstrates individual variance in its association with large scale brain networks and that network topology predicts complex cognitive ability.

Introduction

Social cognition is a construct encompassing many mental processes related to social interaction (Green et al., 2008). Deficits in multiple domains of social cognition are well-described in patients with schizophrenia ((Sprong et al., 2007; Bora et al., 2009; Kohler et al., 2010; Savla et al., 2013; Dodell-Feder et al., 2014; Mehta et al., 2014; Green et al., 2015). These deficits in social cognition may be both partially independent of neurocognitive deficits and are strongly associated with functional status (Allen et al., 2007; Sergi et al., 2007; Fett et al., 2011; Hoe et al., 2012; Mehta et al., 2013; Green, 2016). These findings suggest that social cognitive functioning may be underpinned by neurobiological processes that are at least partially distinct from those associated with other cognitive processes, and contribute uniquely to poor functional outcomes in schizophrenia.

Studies of the neuroanatomical basis of social cognitive deficits using functional magnetic resonance imaging (fMRI) have identified several brain regions associated with various aspects of social processing (see (Green et al., 2015) for review). These include regions involved in emotion processing (i.e. amygdala, inferior occipital gyrus, fusiform gyrus, hippocampal regions, anterior cingulate cortex (ACC), medial prefrontal cortex (mPFC), and inferior frontal and superior temporal gyri) and in theory of mind processing (i.e. left IFG, vmPFC, orbitofrontal cortex, mPFC and temporoparietal junction (Russell et al., 2000; Das et al., 2012; Eack et al., 2013; Dodell-Feder et al., 2014). Notably, the magnitude of the neurobiological abnormality in schizophrenia appears to be associated with measures of real-world social behavior (Dodell-Feder et al., 2014).

Most of these findings come from task-based fMRI studies, which permits effective isolation of specific aspects of social cognitive processes. However, such methods are dependent on task comprehension, effort, and may not be accessible to highly symptomatic clinical populations. Recent studies examining task-free ('resting state') brain connectivity have found network-level abnormalities that are correlated with social cognitive dysfunction (Lynall et al., 2010; Abram et al., 2017). Social cognitive performance in schizophrenia has been associated with abnormal resting state connectivity in medial prefrontal and temporal networks (Carrington and Bailey, 2009; van der Meer et al., 2013; Abram et al., 2017). Disruptions of connectivity in these areas, commonly associated with the default mode network (DMN), have been linked to social cognition and social functioning in patients with SZ (Fox et al., 2017). These findings suggest that even at rest patients

with SZ experience abnormalities in large scale distributed brain networks associated with behavioral and functional measures of social cognition.

In this study, we sought to determine how social cognitive ability is reflected in resting-state brain network connectivity using an unbiased, entirely data-driven approach. We explored the relationship between functional connectivity and performance on a validated, standardized measure of social cognition, from the MATRICS Consensus Cognitive Battery (MCCB) (Nuechterlein et al., 2008). We examined the relationship between social-cognitive performance and functional connectivity at the level of individual brain voxels using multivariate distance matrix regression (MDMR), a technique for connectome-wide association studies (Shehzad et al., 2014). We examined this correlation in a group of over one hundred participants recruited across three distinct sites including individuals with schizophrenia or schizoaffective disorder as well as healthy comparison participants.

Methods

Participants

The study was approved by the Institutional Review Boards of the University of Pittsburgh (Pittsburgh, PA), McLean Hospital (Belmont, MA), and Beth-Israel Deaconess Medical Center (Boston, MA), and all participants gave written informed consent before participating. Participants were recruited from participating health centers using a variety of means including early psychosis treatment programs and community referral networks. Participants at the Boston and Pittsburgh sites were recruited for a clinical trial (BICEPS, NCT01561859). Clinical and imaging data analyzed here was from participants' baseline (pre-intervention) evaluation.

Diagnosis was determined using the Structured Clinical Interview for the DSM-IV (SCID) (First and New York State Psychiatric Institute. Biometrics Research, 2007). Patients were assessed by raters trained in the administration and scoring of the SCID. All participants in the schizophrenia group met DSM-IVTR criteria for the diagnosis of schizophrenia or schizoaffective disorder. Healthy comparison (HC) participants did not meet criteria for any Axis I psychiatric disorder currently or historically.

Exclusion criteria included age outside the range of 18–55, significant neurological disorder, or contraindications to magnetic resonance imaging. IQ<80.

Demographic, clinical, and medication regimen information are summarized in Table 1.

Cognitive Testing

Participant social cognitive performance was assessed using the MATRICS Consensus Cognitive Battery (MCCB) (Nuechterlein et al., 2008). This testing battery includes 7 composite scores of processing speed, attention, working memory, verbal learning, visual learning, problem solving, and social cognition. The social cognition score is calculated from the Mayer-Salovey-Caruso Emotional Intelligence Test (MSCEIT) "managing emotions" subscale (Mayer et al., 2003). The MSCEIT includes a series of vignettes that are read aloud as participants follow along in their own booklets. Participants are then presented with a series of possible actions related to each vignette and asked to assess the effects of each action on the actor's or other characters' mood states or behaviors. Responses are based on a Likert-type scale. We used age and sex normed T scores, which were calculated using the MCCB scoring package.

MRI data acquisition

Boston & Belmont sites: Data were acquired on 3T Siemens Trio (TIM upgrade) scanners using a standard head coil. The echoplanar imaging parameters were as follows: repetition time, 3000 milliseconds; echo time, 30 milliseconds; flip angle, 85°; 3 x 3 x 3-mm voxels; and 47 axial sections collected with interleaved acquisition and no gap. Structural data included a high-resolution T1 image. In addition, all participants underwent a resting fMRI run with the instructions 'remain still, stay awake, and keep your eyes open'. Each functional run lasted 6.2 minutes (124 time points).

Pittsburgh site: Data were acquired on a 3T Siemens Verio scanner using a standard head coil. The echoplanar imaging parameters were as follows: repetition time, 3000 milliseconds; echo time, 30 milliseconds; flip angle, 85°; 3 x 3 x 3-mm voxels; and 45 axial sections collected with interleaved acquisition and no gap. Structural data included a high-resolution T1 image. In addition, all participants underwent a resting fMRI run. Each functional run lasted 6.2 minutes (124 time points).

MRI data processing

The imaging data were preprocessed using DPABI image processing software (Yan et al., 2016). To minimize effects of scanner signal stabilization, the first four images were omitted from all analysis. Scans with head motion exceeding 3 mm or 3° of maximum rotation through the resting-state run were discarded. Functional and structural images were co-registered. Structural images were then normalized and segmented into gray, white and CSF partitions using the DARTEL technique(Ashburner, 2007) A Friston 24-parameter

model(Friston et al., 1996) was used to regress out head motion effects from the realigned data. CSF and white matter signals, global signal as well as the linear trend were also regressed out. After realigning, slice timing correction, and co-registration, framewise displacement (FD) was calculated for all resting state volumes (Power et al., 2012). All volumes with a FD greater than 0.2mm were regressed out as nuisance covariates. Any scan with 50% of volumes removed was discarded. After nuisance covariate regression, the resultant data were band pass filtered to select low frequency (0.01-0.08Hz) signals. Filtered data were normalized by DARTEL into MNI space and then smoothed by a Gaussian kernel of $8mm^3$ full-width at half maximum (FWHM). Voxels within a group derived gray matter mask were used for further analyses.

After preprocessing, a total of 60 participants with schizophrenia or schizoaffective disorder, and 46 HC participants across all sites remained in the study (Table 1).

Functional Connectivity Analysis:

Multivariate Distance Matrix Regression: We performed a connectome-wide association study using multivariate distance matrix regression (MDMR) as originally described in (Shehzad et al., 2014). As has been previously described (Satterthwaite et al., 2015; Shanmugan et al., 2016; Sharma et al., 2017) this analysis occurs in three stages: First, a seed-to-voxel connectivity map is generated by using an individual voxel's BOLD signal timecourse and calculating the Pearson's correlation coefficients between that voxel and all other gray matter voxels. These maps are generated for every participant. In the second stage, the pattern of connectivity is compared among participants using the distance metric $\sqrt{2(1-r)}$. In the third stage, multivariate distance matrix regression tests the relationship between inter-subject differences on a given variable (here MSCEIT score) and inter-subject distances on the connectivity maps generated in stage two. This test results in a pseudo-F statistic for each voxel that demonstrates how MSCEIT score is reflected in functional connectivity at that voxel. This process is repeated for every voxel. Scanner site was included as a covariate in this analysis. Type I error was controlled using a permutation-based cluster correction with a voxel height of $p<.001$ and a cluster extent probability of $p<.05$ (Figure 1A).

This analysis identifies regions of interest (ROI) where MSCEIT score correlates with functional connectivity. The steps of the analysis described above do not display the pattern or direction (i.e. correlation vs anti-correlation) of connectivity that generated the result. To visualize these patterns, it is necessary to conduct post-hoc testing of the regions of interest identified from MDMR. This ROI-based analysis allows

visualization of the connectivity maps that generated the initial result. As others have emphasized (Satterthwaite et al., 2015; Shanmugan et al., 2016; Sharma et al., 2017), these post-hoc tests are not new hypothesis tests, rather, they allow visualization of the connectivity that gave rise to the original MDMR result.

ROI based analyses

For ROI based analyses we used DPABI to extract the time course of the BOLD signal in a given ROI then generated whole brain maps of z-transformed Pearson's correlation coefficients. These maps were entered into SPM12 (Statistical and Parametric Mapping, http://www.fil.ion.ucl.ac.uk/spm). For ROIs generated from MDMR above, we regressed the maps against MSCEIT score to generate maps of how whole brain functional connectivity to the ROIs varies with MSCEIT score. SPM analyses included site as a covariate as in the MDMR analysis; we repeated these analyses with age and sex as additional covariates. To control for movement effects we re-performed these analyses with individual mean FD (framewise displacement) as a subject-level correction for motion effects in all subjects (Power et al., 2012). To control for the effects of medication regimen, the analyses were re-performed with CPZE as a covariate within the schizophrenia/schizoaffective group .

For other, subsequent ROI based connectivity analyses described below, we used DPABI to calculate the time course of the average BOLD signal in a sphere, and then generated whole brain maps of z-transformed Pearson's correlation coefficients. We then used SPM12 to generate single-sample t-tests of these connectivity maps.

Structural MRI Analysis:

Structural MPRAGE images were checked for artifacts and were processed using Freesurfer 6 (http://surfer.nmr.mgh.harvard.edu/). The images went through first-level auto-reconstruction to register the scans in standard space and skull strip the brains. One rater (OL) edited the images to remove dura, sinuses and vessels that could interfere with segmentation. After visual inspection, 98 images were retained for analysis. The images then went through second and third level auto-reconstruction to register the brains to the Desikan-Killiany atlas and extract sulcal depth measurements (Desikan et al., 2006). Sulcal depth in Freesurfer is the integrated dot product of the movement vector and the surface normal during inflation. Deep regions therefore are expressed as positive values as they move outwards while more superficial regions move inwards. Units are the standard deviation from the median value.

Table and figure generation

Graphs of relationships between social cognitive ability and structural/functional measures were generated using R. Projections of ROIs and T contrast maps onto cortical surfaces was accomplished using FSL (Jenkinson et al., 2012) and Caret (Van Essen et al., 2001).

Results

Functional Connectivity in the Superior Parietal Lobule Predicts Social Cognitive Ability

MDMR analysis revealed a single region whose intrinsic functional connectivity correlated significantly with social cognition score. This identified a (59 voxel) region in the left superior parietal lobule (SPL) centered at MNI coordinates X-24 y-69 z57 (Figure 1B).

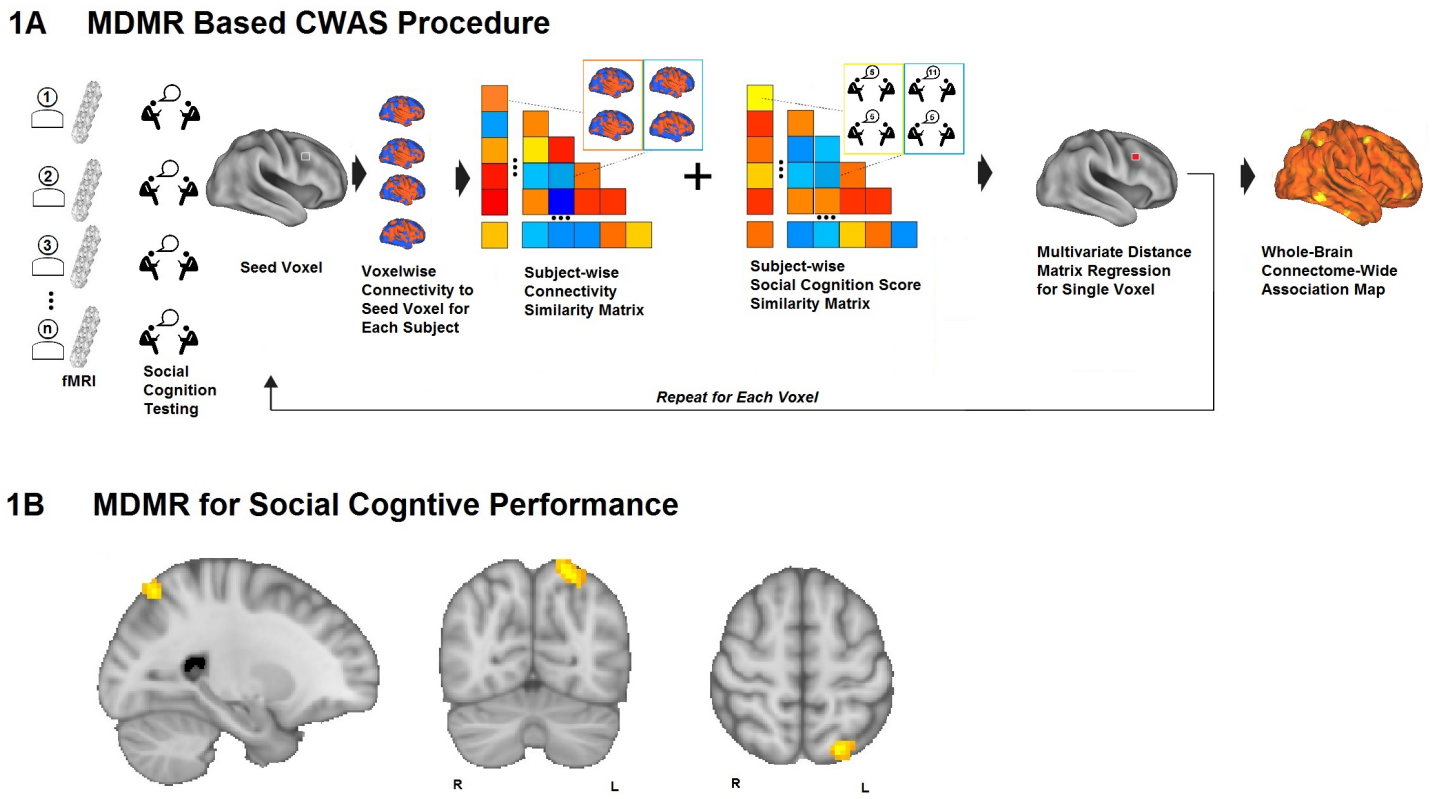

Figure 1.

Multivariate Distance Matrix Regression identifies brain voxels whose functional connectivity varies with performance on a measure of social cognitive ability.
1A. MDMR procedure: rsfMRI and social cognitive ability scores are collected from each participant. For each participant a functional connectivity map is generated to an individual voxel. The pattern of connectivity is compared among participants using a distance metric. Next, multivariate distance matrix regression tests the relationship between inter-subject differences on social cognitive performance and inter-subject distances on the functional connectivity maps. This test results in a pseudo-F statistic for each voxel that demonstrates how social cognition is reflected in functional connectivity at that voxel. This process is repeated for every voxel.

1B. In our sample of 106 participants (n=60 with schizophrenia or schizoaffective disorder and n= 46 HC participants), we identified a single region in the left superior parietal lobule (extent k=59, centered at MNI coordinates X-24 y-69 z57) whose connectivity correlated significantly with social cognition score. Connectivity is thresholded at a voxelwise level of $p<.001$ and extent threshold of $p<.05$.

SPL Association with Distributed Brain Networks Predicts Social Cognitive Ability

We performed Post-hoc testing using this region as a ROI to determine the distribution and directionality of connectivity that gave rise to this result. This analysis revealed two apparent patterns of functional connectivity: Higher social cognitive ability correlated with increasing intrinsic connectivity between this region and bilateral fronto-parietal and temporal regions that correspond to the canonical "default mode network" (DMN) (Figure 2A). Lower social cognitive ability correlated with increasing functional connectivity between this region and bilateral parietal-occipital regions that mirror the canonical distribution of the "dorsal attention network" (DAN) (Figure 2B). This result remained significant with the inclusion of sex and age as covariates and was significant with individual motion (FD) included as a covariate.

Given significant concerns about the replicability of fMRI imaging studies, we sought to determine if these findings could be observed in each study population (Boston/Pittsburgh and McLean Hospital) independently to better confirm the replicability of this result. Both study populations independently observe the same pattern of SPL functional connectivity correlating with social cognition (i.e. DMN connectivity with higher social cognitive ability and DAN connectivity with lower social cognitive ability) (Supplemental Figure 1).

We plotted the relationship between social cognition and functional connectivity for both networks as a scatter plot in Figure 2C & 2D. As expected from the maps in Figure 2A & 2B, we observed that higher social cognitive ability was correlated with increased functional connectivity between the SPL and the DMN and decreased connectivity to the DAN. Because the DMN is intrinsically anti-correlated with the DAN, this result could be expected for any region in one of these networks (i.e. a region of interest located in the distribution of the DMN that demonstrated lower correlation to the rest of the DMN would be expected to demonstrate higher correlation to the DAN). Surprisingly, the scatter plots of connectivity cross the axis of 0 connectivity i.e. *this SPL region is intrinsically connected to the DMN in some individuals and is intrinsically connected to the DAN in others*.

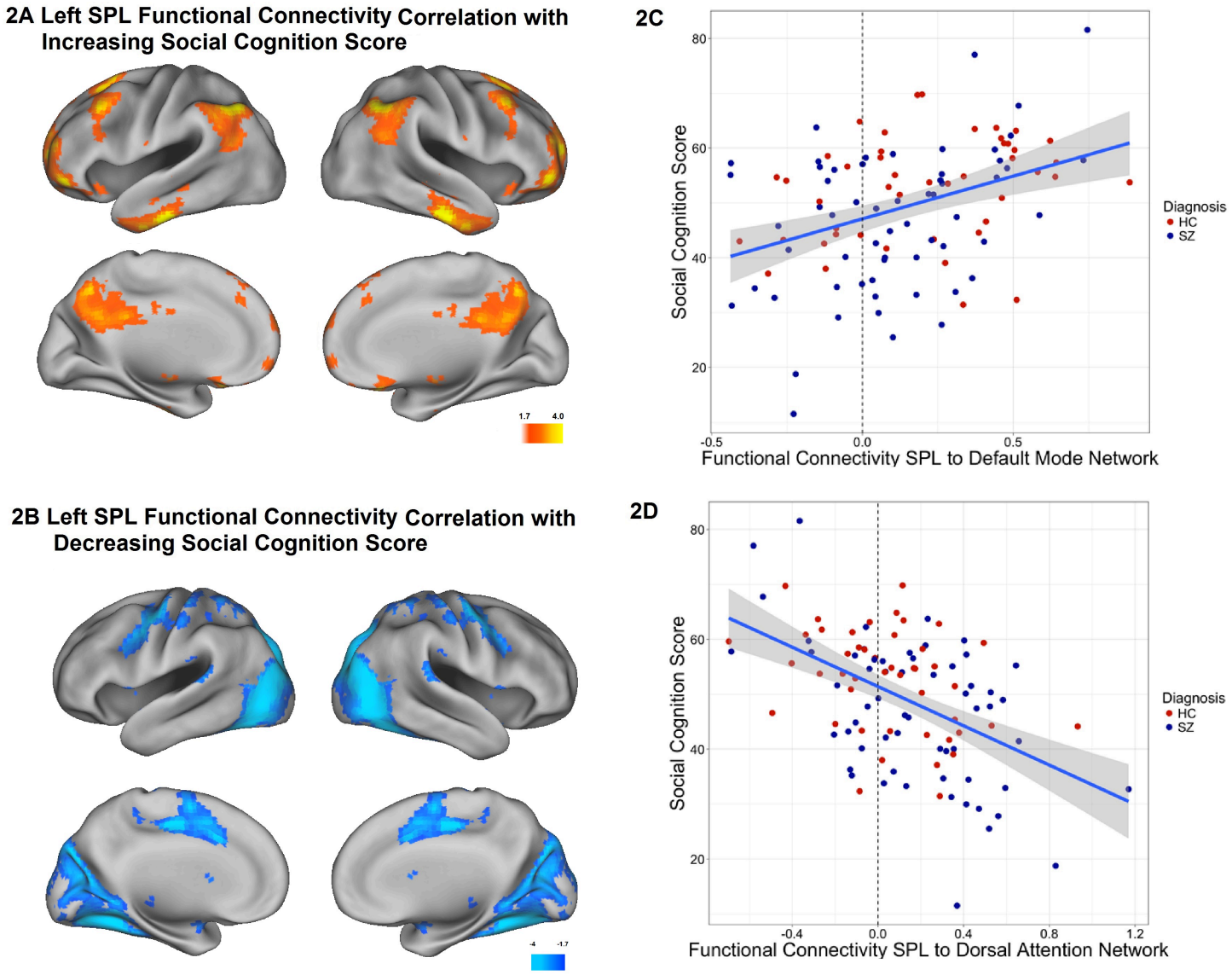

Figure 2.

Post-hoc testing to determine the pattern and directionality of connectivity that gave rise to the MDMR result. Two patterns of connectivity are observed. **2A**. Social cognition score is correlated with functional connectivity between the left SPL region and the "default mode network" (DMN). **2B.** Social cognition score is inversely correlated with functional connectivity between the left SPL and the "dorsal attention network" (DAN). Color bar: T-statistic. **2C**. Plot of social cognition score (y-axis) and functional connectivity between 6mm sphere at SPL ROI coordinates (X-24 y-69 z57) and 6mm sphere at the region of maximally correlated connectivity in the DMN (x12 y-87 z-30) (x-axis). **2D.** Plot of social cognition score (y-axis) and functional connectivity between 6mm sphere at SPL ROI coordinates X-24 y-69 z57 and 6mm sphere at the region of maximal inversely correlated connectivity in the DAN (x36 y-78 z21) (x-axis). Notably, both graphs demonstrate correlations that cross the reference line of null functional connectivity, meaning that this ROI does not simply display cognition-connectivity correlations within the DMN and expected cognition-connectivity anti-correlations in the network (DAN) anti-correlated with the DMN. Rather, the network association of this region appears to shift from being a member of the DMN to a member of the DAN as one moves along the distribution from higher scoring individuals to lower scoring individuals.

Network Toploogy Predicts Social Cognitive Ability

In order to investigate the relationship between cognition and inter-individual variance in network topography, we performed an exploratory post-hoc analysis to visualize intrinsic connectivity to this region in subsets of participants. We performed one-sample T-tests among the participants with the highest and lowest social cognitive ability. In this analysis, we examined intrinsic SPL connectivity among participants top 5th percentile of social cognitive performance and participants in the bottom 5th percentile of social cognitive performance. Using this analysis, the SPL ROI in the top 5th percentile scorers showed connectivity with the canonical DMN. In the bottom 5th percentile, this ROI was a member of the DAN (figure 3A).

To better place this finding in the context of existing studies of the DMN, we compared the topology of the DMN in the individuals with the highest social cognitive performance and those with the lowest using canonical methods for identifying the DMN (figure 3B). We placed a 10mm spherical ROI in the precuneus to visualize the distribution of the DMN and a 10 mm spherical ROI in the frontal eye fields to visualize the DAN. As expected from the results in figures 2 & 3A, we observe that, in the highest scoring individuals, the SPL ROI is included in the topology of their DMN and in the lowest scoring individuals, the SPL ROI is included in the DAN.

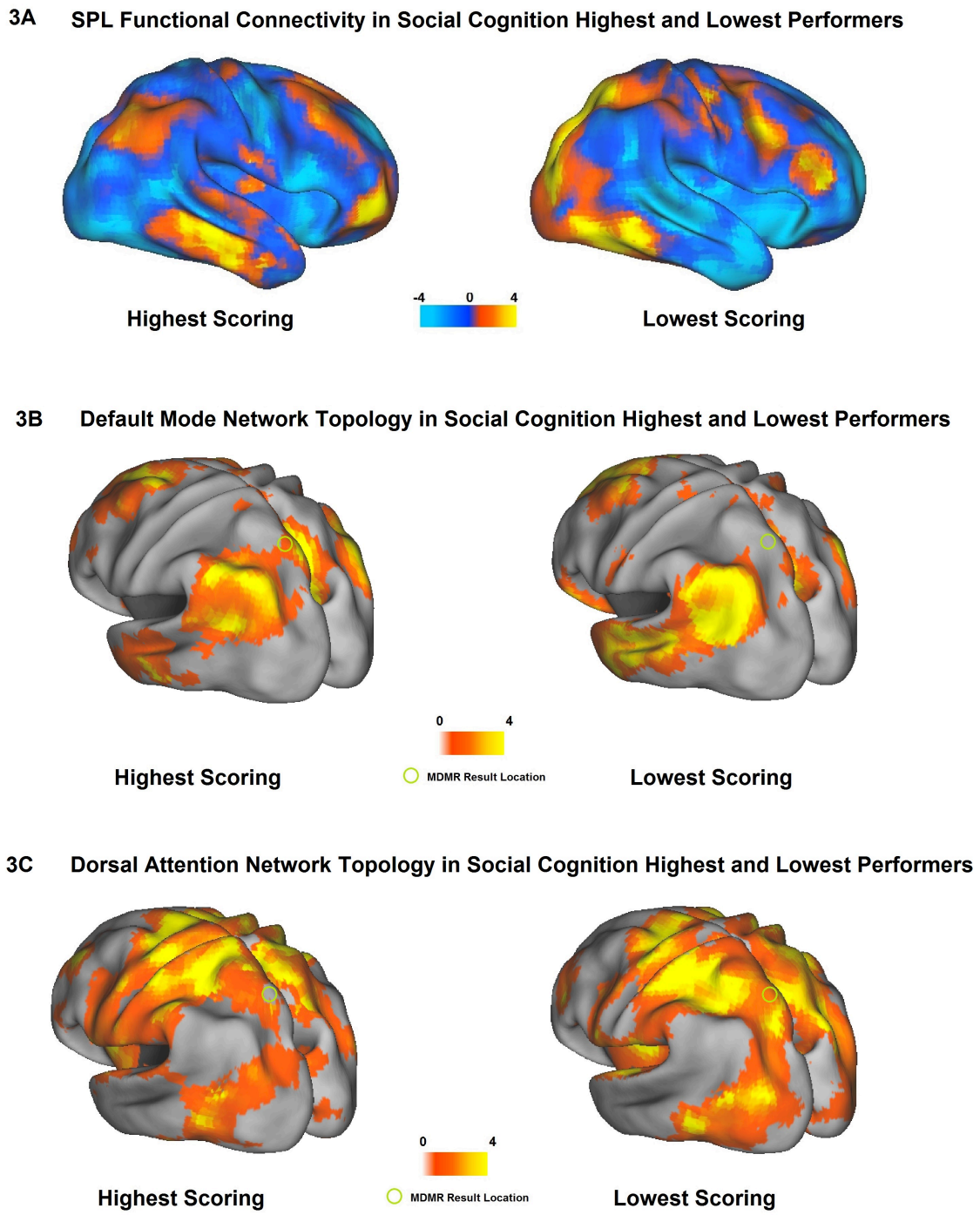

Figure 3.

The left SPL ROI is connected to different brain networks in participants with high versus low social cognitive ability. Here we visually confirm the implication of the cognition-connectivity correlations shown in 2C and 2D by looking at absolute connectivity in the highest and lowest scorers on social cognitive testing.
3A One sample T-tests of functional connectivity to the Left SPL ROI in the participants in the top 5th percentile of social cognition performance and the participants in the bottom 5th percentile. In the highest scoring individuals, the SPL ROI is correlated with the DMN and anti-correlated with the DAN. In the lowest scoring individuals, the SPL ROI is correlated with DAN and anti-correlated with DMN. Color bar = T-statistic.
3B & 3C The topographic distribution of the Default Mode Network and Dorsal Attention Network as visualized using canonical methods: The topographic distribution of the DMN is derived from functional connectivity to a 10mm spherical ROI placed in the precuneus (x-4, y-58, z44) and the DAN from a 10mm sphere ROI placed in

the frontal eye fields (x28 y-8, z52). Consistent with the results of 3A above, we observe significant variability in the topology of both networks with their inclusion or exclusion of the SPL ROI predicting social cognitive ability.

As an exploratory analysis, we asked if the network connectivity of the SPL region predicted cognition broadly or was specific to social cognition. We examined connectivity to this ROI regressed against social cognition score with full scale IQ (FSIQ) as a covariate. This was performed on participants in the study with FSIQ data available (BICEPS i.e. Pittsburgh and Boston). In this analysis, we again observed the same pattern of social cognition correlated functional connectivity as seen without FSIQ as a covariate (Supplementary Figure 2).

We examined functional connectivity-social cognition relationships in HC participants and those with schizophrenia/schizoaffective disorder independently. Using the same ROIs as in figure 2C & 2D, we correlated FC with social cognitive performance. We observe similar strengths of correlation between social cognitive performance and DMN-SPL connectivity in HC (R=.329, p=.026) and schizophrenia (R= .377, p=.003) populations and also see similar correlation strengths in DAN-SPL connectivity in HC (R=-.445, p=.002) and schizophrenia populations (R=-.504, p<.001).

Sulcal Depth at the SPL Correlates with Social Cognitive Ability

Prior studies have revealed considerable individual variation at the cytoarchitectonic level in this region (see discussion). This level of analysis is not available but we asked whether there is a structural MRI correlate to network connectivity and social cognitive ability in this region? Based on prior studies of structural variability in this region (Mueller et al., 2013), and the suggestion that the intraparietal sulcus area hIP3 may be associated with a DMN-like pattern of connectivity (Wang et al., 2015b), we hypothesized that social cognitive ability would be correlated with sulcal depth in this region. As predicted, we observed a significant (r=0.269, *p*=0.0075) relationship between sulcal depth and social cognitive ability (Figure 4).

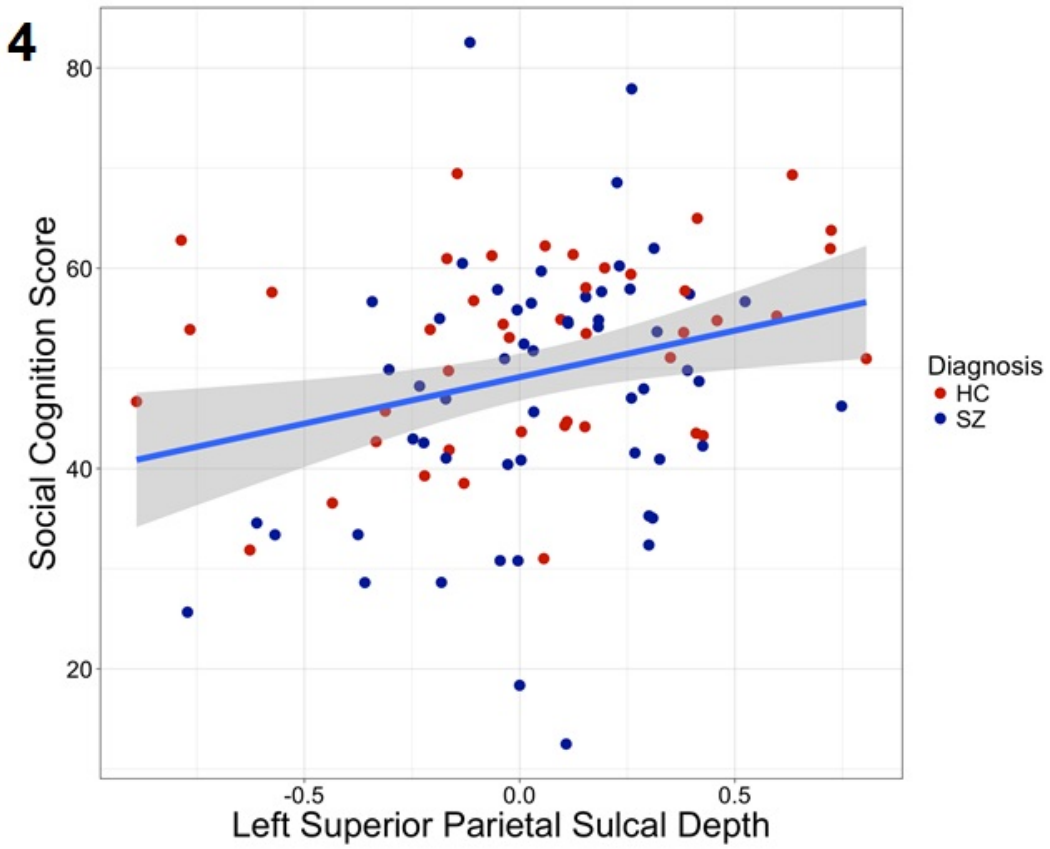

Figure 4

Social cognitive ability is correlated with sulcal depth in the left SPL. The Freesurfer program was used to conduct a ROI based analysis of sulcal depth in the left superior parietal lobule. These values were then correlated with individual social cognition scores. Units are standard deviations from the median. This analysis revealed a significant correlation between sulcal depth and social cognitive ability (r=0.269, *p*=0.0075).

Discussion

We here identify a region of the left superior parietal lobule whose intrinsic functionally connectivity correlates significantly with social cognitive ability. Surprisingly, the relationship between connectivity and cognition appears to be mediated by topography.. Specifically, this region is variably connected to two large scale brain networks, the DMN and the DAN. The brain is organized into networks (Buckner et al., 2011; Power et al., 2011) Individual variation in network topology has been demonstrated previously(Mueller et al., 2013; Laumann et al., 2015; Poldrack et al., 2015; Wang et al., 2015a; Gordon et al., 2017a; Gordon et al., 2017b). To date however, this variability in network topology has not been associated with behavioral or cognitive phenotypes. In our study population, social cognitive ability is predicted by brain network membership: In high performers, spontaneous activity this region is correlated with the default mode network and anti-correlated with the dorsal attention network. This network membership is reversed in low performers.

What is the basis of this variability in network membership of the SPL? A convergence of results from multiple research methods have demonstrated that the SPL can be subdivided into at least four distinct subregions that are differentiable on the basis of cytoarchitectonic description (Scheperjans et al., 2008), white matter tractography (Mars et al., 2011), and both task evoked and resting state functional connectivity (Wang et al., 2015b). Particularly relevant to this study is the finding that postmortem cytoarchitectonic studies identified considerable individual heterogeneity in the SPL (Scheperjans et al., 2008). The topographical distribution of these subregions in the left SPL was observed to show significant inter-subject variability, particularly in the region referred to as area 7A whose center of gravity corresponds to the region identified in this study.

Using group-averaged functional connectivity maps of the SPL Wang et al. observed specific patterns of resting state connectivity to left SPL subregions (Wang et al., 2015b). That study identified five different “clusters” of resting state connectivity to the left SPL. Notably, the adjacent “L3 and L4” regions in that manuscript demonstrate specific connectivity patterns similar to the DMN and DAN patterns we observe among social cognition high and low performers respectively. These regions appear to correspond to the hIP3 & 7A regions respectively, identified by Scheperjans et al. (Scheperjans et al., 2008). Moving outside of these regions, when we examine connectivity at coordinates that correspond to the other SPL subdivisions i.e. the Scheperjans 5L / Wang L2 region rostral to the MDMR ROI or the Scheperjans 7P / Wang L5 caudal to the

MDMR ROI, we do not see a correlation between connectivity and social cognitive ability (Supplemental Materials text and Supplemental Figure 3).

We hypothesize that the individual variability in resting state connectivity in this ROI identified by MDMR represents individual variability in the cytoarchitectonic organization of the left SPL. Furthermore, we hypothesize that the correlation between network connectivity and social cognitive ability is a cognitive correlate of this anatomic variability. To date, studies have not linked cytoarchitectonic variation in the SPL to cognitive variation. In support of this hypothesis, one existing study has correlated diffusion tensor imaging measures with performance on the same social cognition test used in this study. In that article, Pisner et al. observed social cognitive performance correlating with increased fractional anisotropy in the cingulum connecting frontal and parietal regions in a distribution entirely consistent with our observation of social cognition correlating with fronto-parietal connectivity (Pisner et al., 2017).

There is converging evidence suggesting that the DMN has a particular role in social intelligence (Mars et al., 2012; Fox et al., 2017). The DMN is a large, distributed brain network. Why does such a circumscribed region of this network in the superior parietal lobule appear to be such a critical determinant of social cognitive ability? A neuroanatomical model called the parieto-frontal integration theory (P-FIT) suggests that connectivity between parietal cortex and frontal areas is a critical determinant of intelligence(Jung and Haier, 2007). In this specific scenario, connectivity between the parietal lobule and a parieto-frontal network implicated in social intelligence (the DMN) may mediate social cognition...

In our study, the relationship between SPL network membership and social cognitive performance was trans-diagnostic and is observed in both participants with schizophrenia and schizoaffective disorder as well as HC participants. This is observed despite a representative patient sample in which the mean social cognition performance was significantly less than that of HC participants (p=.015). We hypothesize that what is already known about schizophrenia network pathophysiology may explain social cognition deficits in this disorder. There is evidence that the molecular pathophysiology believed to underlie schizophrenia leads to the selective disruption of fronto-parietal networks (e.g. the DMN) that is a hallmark feature of schizophrenia and related disorders (Baker et al., 2014; Yang et al., 2016). If social cognitive ability is partially dependent on left SPL connectivity to an intact DMN, our result may provide a mechanistic bridge linking a “synaptic” disease to poor societal functioning.

Limitations of this study include the fact the social cognition measure included in the MCCB does not individually test every sub-process involved in social cognition (e.g. social perception, theory of mind, attributional bias etc.) (Eack et al., 2010). In addition, as with other cohort imaging studies, this study is inherently correlational and cannot distinguish between connectivity directly mediating cognition versus other interpretations e.g. the result of an underlying process that mediates social cognitive ability and network connectivity via unrelated processes.

Ultimately, interventions designed to improve social cognition that incorporate imaging will validate or refute this network-based model of social cognition by measuring network connectivity longitudinally before and after interventions to improve social cognitive performance. This may be particularly relevant for behavioral clinical trials that utilize a “target engagement” framework to validate experimental therapeutics (Lewandowski et al., 2017). In that vein, the location of our result provides a potential target for neuromodulation. For example, If the network “membership” of this region can be modified via induction of neuroplasticity at this region (e.g. by repetitive transcranial magnetic stimulation), then neuromodulation may enhance trials using cognitive remediation interventions.

More generally, the utility of this result extends beyond imaging studies of social cognition. The demonstration that individual brain network topology is associated with individual variation in complex cognition reinforces a growing appreciation of the limitations of group-based averaging in resting-state imaging. Averaging across groups of subjects likely obfuscates relationships between individual network topology and cognitive and behavioral phenotypes. In this example, the relationship between network topology and cognitive measures was significant enough to be discerned in a group of a hundred subjects scanned a single time each. It seems inevitable that other relationships between network topology and cognition / behavior remain to be discovered but discerning those relationships may likely require “dense” scanning of individual subjects i.e. scanning the same individuals five (Mueller et al., 2013), twelve(Gordon et al., 2017b), or twenty-four times (Braga and Buckner, 2017). Such efforts are resource intensive, but if such deep characterization yields greater understanding of network-behavior relationships, it is reasonable to imagine a re-allocation of resources away from participant numbers and towards precise network mapping. A remaining challenge to be addressed is how such a change in approach may be applied to better understand the network basis of

neurological and psychiatric disorders where acquiring multiple scans in symptomatic individuals may prove difficult.

Demographics

	Mclean (n=45)	
	Probands (n=16)	**Healthy Controls (n=29)**
Age (SD)	28.38 (9.31)	25.90 (6.77)
Sex	1 Female, 15 Males	18 Females, 11 Males
Race	2 African American 4 Asian 10 Caucasian	1 African American 3 Asian 24 Caucasian 1 Other
Diagnosis	16 Schizophrenia	N/A
CPZE (SD)	248.95 (154.75)	N/A

	Pittsburgh (n=39)	
	Probands (n=22)	**Healthy Controls (n=17)**
Age (SD)	29.31 (4.80)	28.15 (3.99)
Sex	10 Female, 12 Males	5 Females, 12 Males
Race	6 African American 2 Asian 1 Hispanic 13 Caucasian	4 African Americans 1 Asian 12 Caucasian
Diagnosis	17 Schizophrenia 5 Schizoaffective	N/A
CPZE (SD)	292.55 (171.18)	N/A

	Boston (n=22)	
	Probands (n=22)	**Healthy Controls (n=0)**
Age (SD)	27.21 (4.05)	N/A
Sex	5 Female, 17 Males	N/A
Race	1 Asian 14 Caucasian 3 Multi 4 Other	N/A
Diagnosis	18 Schizophrenia 4 Schizoaffective	N/A
CPZE (SD)	318.05 (284.91)	N/A

Table 1

Participant demographics and clinical information. Abbreviations: CPZE chlorpromazine equivalents

SD Standard Deviation

Supplementary Materials

SF1

BICEPS Participants

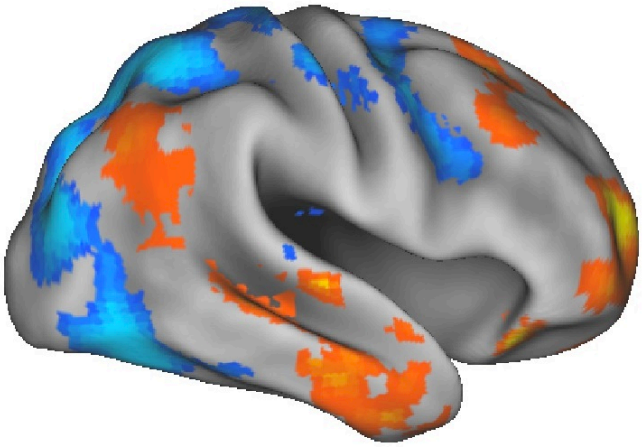

McLean Hospital Participants

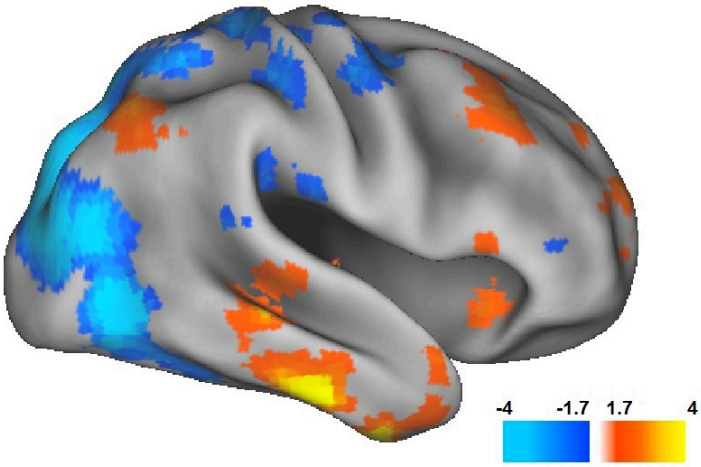

Supplemental Figure 1.

Post-hoc testing of social cognition / functional connectivity correlations in each study population. The same pattern of correlations between left SPL connectivity and social cognition score are observed at the McLean and Boston/Pittsburgh (BICEPS) samples independently. Color bar = T-statistic.

SF2 Social Cognition-SPL connectvity with FSIQ as covariate

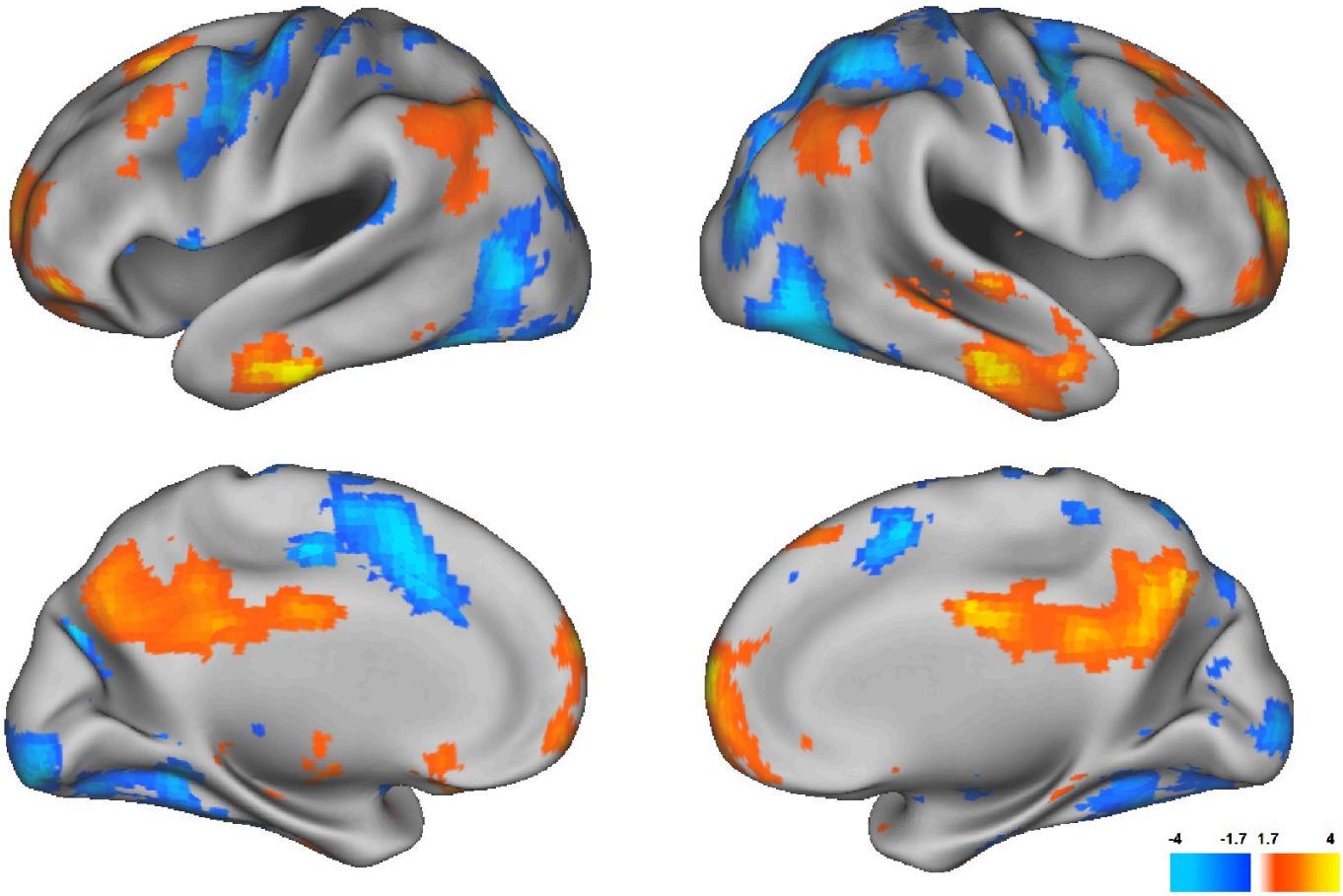

Supplemental Figure 2.

The functional connectivity of the SPL region regressed against social cognitive performance with full scale IQ (FSIQ) as a covariate. In an analysis of the sites with FSIQ available (Pittsburgh and Boston), we continue to observe the same pattern of SPL connectivity-social cognition correlations. Color bar = T-statistic.

The relationship between functional connectivity and social cognition is SPL subdivision specific.

MDMR identifies regions whose functional connectivity correlates significantly with a given variable, in this case social cognition score. Adjacent SPL subdivisions were not identified as regions with significant correlation between social cognitive ability and functional connectivity. To better visualize these negative results in adjacent SPL subdivisions, we conducted one-sample connectivity analyses to ROIs in SPL subdivisions just rostral and caudal to the region identified by MDMR. We placed 6mm spherical ROIs at coordinates that correspond to adjacent but cytoarchitectonically distinct regions of the parietal lobe (rostral MNI coordinates x-21 y-55 z72, corresponding to Scheperjans 5L / Wang L2 and caudal MNI coordinates x-24 y-69 z57, corresponding to Scheperjans 7P / Wang L5 (Scheperjans et al., 2008; Wang et al., 2015b).

We examined the intrinsic connectivity of these ROIs and compared them to the ROI identified by MDMR. While participants with high social cognitive ability were readily distinguished from low performers on the basis of connectivity to the MDMR ROI, in the adjacent SPL subdivisions both groups demonstrated largely overlapping connectivity in patterns consistent with previously published results (Wang et al., 2015b) (Supplementary Figure 4). Only the ROI corresponding to the MDMR result demonstrated a relationship between social cognitive ability and network “membership” i.e. connectivity to DMN versus DAN.

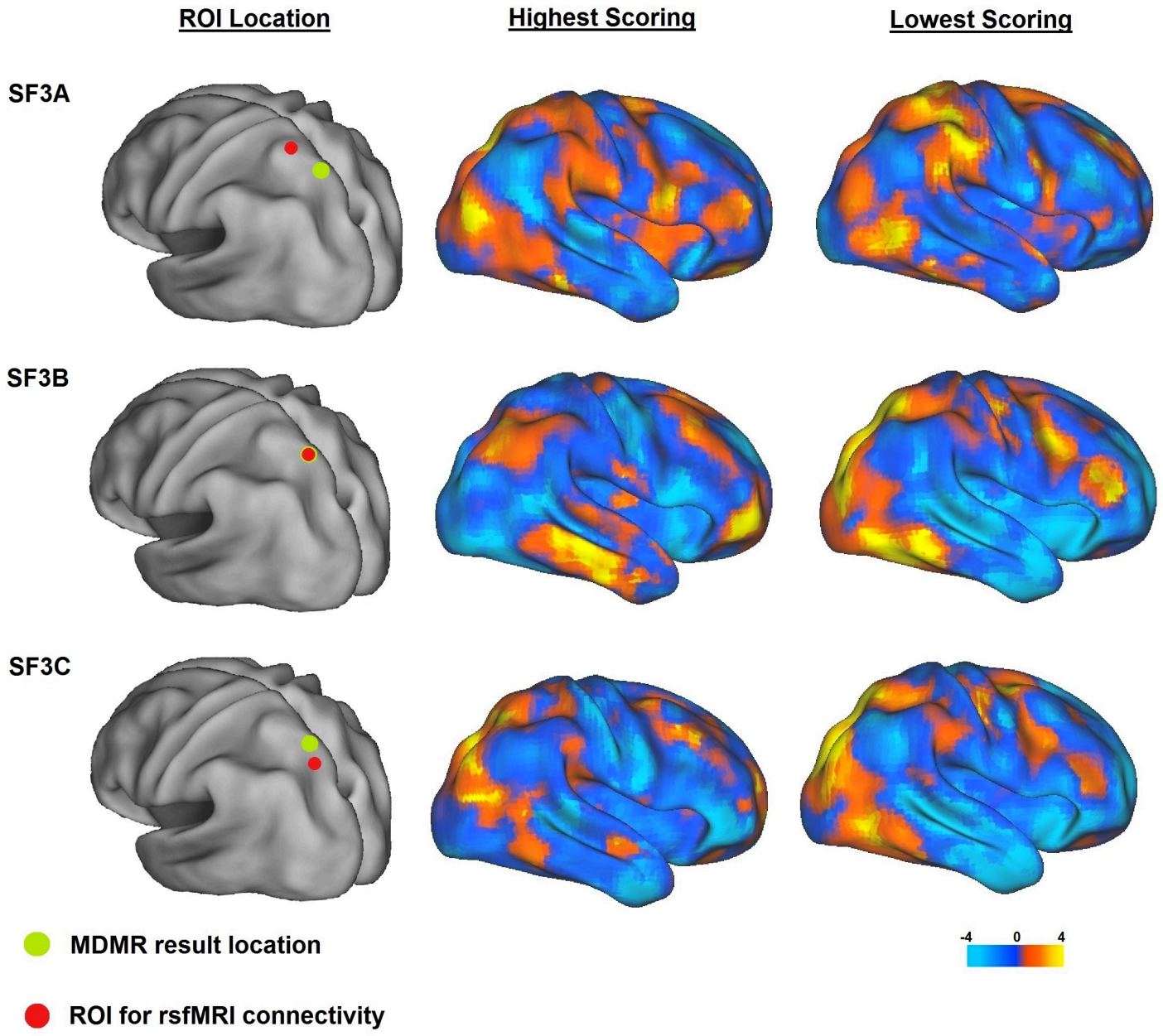

Supplementary Figure 3.

The relationship between functional connectivity and social cognition is SPL subdivision specific. One sample T-tests of functional connectivity to three adjacent superior parietal ROIs in the participants in the top 5th percentile of social cognitive performance and the participants in the bottom 5th percentile of social cognitive performance. These three ROIs are: **SF3A**. 6mm sphere rostral to the MDMR result (SPL region 5L/L2, MNI x-21 y-55 z72). **SF3B.** The MDMR result (MNI x-24 y-69 z57), and **SF3C.** 6mm sphere caudal to the MDMR result (at SPL region 7P/L5, MNI x-16 y-75 z50). Functional connectivity to the MDMR result ROI shows distinct patterns of functional connectivity in the highest and lowest performers in social cognition. The rostral and caudal ROIs demonstrate patterns of connectivity that are largely overlapping between highest and lowest performers on social cognitive testing.

References

Abram SV, Wisner KM, Fox JM, Barch DM, Wang L, Csernansky JG, MacDonald AW, 3rd, Smith MJ (2017) Fronto-temporal connectivity predicts cognitive empathy deficits and experiential negative symptoms in schizophrenia. Hum Brain Mapp 38:1111-1124.

Allen DN, Strauss GP, Donohue B, van Kammen DP (2007) Factor analytic support for social cognition as a separable cognitive domain in schizophrenia. Schizophr Res 93:325-333.

Ashburner J (2007) A fast diffeomorphic image registration algorithm. Neuroimage 38:95-113.

Baker JT, Holmes AJ, Masters GA, Yeo BT, Krienen F, Buckner RL, Ongur D (2014) Disruption of cortical association networks in schizophrenia and psychotic bipolar disorder. JAMA psychiatry 71:109-118.

Bora E, Yucel M, Pantelis C (2009) Cognitive endophenotypes of bipolar disorder: a meta-analysis of neuropsychological deficits in euthymic patients and their first-degree relatives. J Affect Disord 113:1-20.

Braga RM, Buckner RL (2017) Parallel Interdigitated Distributed Networks within the Individual Estimated by Intrinsic Functional Connectivity. Neuron 95:457-471 e455.

Buckner RL, Krienen FM, Castellanos A, Diaz JC, Yeo BT (2011) The organization of the human cerebellum estimated by intrinsic functional connectivity. J Neurophysiol 106:2322-2345.

Carrington SJ, Bailey AJ (2009) Are there theory of mind regions in the brain? A review of the neuroimaging literature. Hum Brain Mapp 30:2313-2335.

Das P, Lagopoulos J, Coulston CM, Henderson AF, Malhi GS (2012) Mentalizing impairment in schizophrenia: a functional MRI study. Schizophr Res 134:158-164.

Desikan RS, Segonne F, Fischl B, Quinn BT, Dickerson BC, Blacker D, Buckner RL, Dale AM, Maguire RP, Hyman BT, Albert MS, Killiany RJ (2006) An automated labeling system for subdividing the human cerebral cortex on MRI scans into gyral based regions of interest. Neuroimage 31:968-980.

Dodell-Feder D, Delisi LE, Hooker CI (2014) The relationship between default mode network connectivity and social functioning in individuals at familial high-risk for schizophrenia. Schizophr Res 156:87-95.

Eack SM, Wojtalik JA, Newhill CE, Keshavan MS, Phillips ML (2013) Prefrontal cortical dysfunction during visual perspective-taking in schizophrenia. Schizophr Res 150:491-497.

Eack SM, Greeno CG, Pogue-Geile MF, Newhill CE, Hogarty GE, Keshavan MS (2010) Assessing social-cognitive deficits in schizophrenia with the Mayer-Salovey-Caruso Emotional Intelligence Test. Schizophrenia bulletin 36:370-380.

Fett AK, Viechtbauer W, Dominguez MD, Penn DL, van Os J, Krabbendam L (2011) The relationship between neurocognition and social cognition with functional outcomes in schizophrenia: a meta-analysis. Neurosci Biobehav Rev 35:573-588.

First MB, New York State Psychiatric Institute. Biometrics Research D (2007) Structured clinical interview for DSM-IV-TR axis I disorders : SCID-I. New York, N.Y.: Biometrics Research Dept., New York State Psychiatric Institutute.

Fox JM, Abram SV, Reilly JL, Eack S, Goldman MB, Csernansky JG, Wang L, Smith MJ (2017) Default mode functional connectivity is associated with social functioning in schizophrenia. J Abnorm Psychol 126:392-405.

Friston KJ, Williams S, Howard R, Frackowiak RS, Turner R (1996) Movement-related effects in fMRI time-series. Magn Reson Med 35:346-355.

Gordon EM, Laumann TO, Adeyemo B, Gilmore AW, Nelson SM, Dosenbach NUF, Petersen SE (2017a) Individual-specific features of brain systems identified with resting state functional correlations. Neuroimage 146:918-939.

Gordon EM, Laumann TO, Gilmore AW, Newbold DJ, Greene DJ, Berg JJ, Ortega M, Hoyt-Drazen C, Gratton C, Sun H, Hampton JM, Coalson RS, Nguyen AL, McDermott KB, Shimony JS, Snyder AZ, Schlaggar BL, Petersen SE, Nelson SM, Dosenbach NUF (2017b) Precision Functional Mapping of Individual Human Brains. Neuron 95:791-807 e797.

Green MF (2016) Impact of cognitive and social cognitive impairment on functional outcomes in patients with schizophrenia. J Clin Psychiatry 77 Suppl 2:8-11.

Green MF, Horan WP, Lee J (2015) Social cognition in schizophrenia. Nature reviews Neuroscience 16:620-631.

Green MF, Penn DL, Bentall R, Carpenter WT, Gaebel W, Gur RC, Kring AM, Park S, Silverstein SM, Heinssen R (2008) Social cognition in schizophrenia: an NIMH workshop on definitions, assessment, and research opportunities. Schizophrenia bulletin 34:1211-1220.

Hoe M, Nakagami E, Green MF, Brekke JS (2012) The causal relationships between neurocognition, social cognition and functional outcome over time in schizophrenia: a latent difference score approach. Psychol Med 42:2287-2299.

Jenkinson M, Beckmann CF, Behrens TE, Woolrich MW, Smith SM (2012) Fsl. Neuroimage 62:782-790.

Jung RE, Haier RJ (2007) The Parieto-Frontal Integration Theory (P-FIT) of intelligence: converging neuroimaging evidence. Behav Brain Sci 30:135-154; discussion 154-187.
Kohler CG, Walker JB, Martin EA, Healey KM, Moberg PJ (2010) Facial emotion perception in schizophrenia: a meta-analytic review. Schizophrenia bulletin 36:1009-1019.
Laumann TO, Gordon EM, Adeyemo B, Snyder AZ, Joo SJ, Chen MY, Gilmore AW, McDermott KB, Nelson SM, Dosenbach NU, Schlaggar BL, Mumford JA, Poldrack RA, Petersen SE (2015) Functional System and Areal Organization of a Highly Sampled Individual Human Brain. Neuron 87:657-670.
Lewandowski KE, Ongur D, Keshavan MS (2017) Development of novel behavioral interventions in an experimental therapeutics world: Challenges, and directions for the future. Schizophr Res.
Lynall ME, Bassett DS, Kerwin R, McKenna PJ, Kitzbichler M, Muller U, Bullmore E (2010) Functional connectivity and brain networks in schizophrenia. J Neurosci 30:9477-9487.
Mars RB, Neubert FX, Noonan MP, Sallet J, Toni I, Rushworth MF (2012) On the relationship between the "default mode network" and the "social brain". Front Hum Neurosci 6:189.
Mars RB, Jbabdi S, Sallet J, O'Reilly JX, Croxson PL, Olivier E, Noonan MP, Bergmann C, Mitchell AS, Baxter MG, Behrens TE, Johansen-Berg H, Tomassini V, Miller KL, Rushworth MF (2011) Diffusion-weighted imaging tractography-based parcellation of the human parietal cortex and comparison with human and macaque resting-state functional connectivity. J Neurosci 31:4087-4100.
Mayer JD, Salovey P, Caruso DR, Sitarenios G (2003) Measuring emotional intelligence with the MSCEIT V2.0. Emotion 3:97-105.
Mehta UM, Bhagyavathi HD, Thirthalli J, Kumar KJ, Gangadhar BN (2014) Neurocognitive predictors of social cognition in remitted schizophrenia. Psychiatry Res 219:268-274.
Mehta UM, Thirthalli J, Subbakrishna DK, Gangadhar BN, Eack SM, Keshavan MS (2013) Social and neuro-cognition as distinct cognitive factors in schizophrenia: a systematic review. Schizophr Res 148:3-11.
Mueller S, Wang D, Fox MD, Yeo BT, Sepulcre J, Sabuncu MR, Shafee R, Lu J, Liu H (2013) Individual variability in functional connectivity architecture of the human brain. Neuron 77:586-595.
Nuechterlein KH et al. (2008) The MATRICS Consensus Cognitive Battery, part 1: test selection, reliability, and validity. Am J Psychiatry 165:203-213.
Pisner DA, Smith R, Alkozei A, Klimova A, Killgore WD (2017) Highways of the emotional intellect: white matter microstructural correlates of an ability-based measure of emotional intelligence. Soc Neurosci 12:253-267.
Poldrack RA et al. (2015) Long-term neural and physiological phenotyping of a single human. Nat Commun 6:8885.
Power JD, Barnes KA, Snyder AZ, Schlaggar BL, Petersen SE (2012) Spurious but systematic correlations in functional connectivity MRI networks arise from subject motion. Neuroimage 59:2142-2154.
Power JD, Cohen AL, Nelson SM, Wig GS, Barnes KA, Church JA, Vogel AC, Laumann TO, Miezin FM, Schlaggar BL, Petersen SE (2011) Functional network organization of the human brain. Neuron 72:665-678.
Russell TA, Rubia K, Bullmore ET, Soni W, Suckling J, Brammer MJ, Simmons A, Williams SC, Sharma T (2000) Exploring the social brain in schizophrenia: left prefrontal underactivation during mental state attribution. Am J Psychiatry 157:2040-2042.
Satterthwaite TD, Vandekar SN, Wolf DH, Bassett DS, Ruparel K, Shehzad Z, Craddock RC, Shinohara RT, Moore TM, Gennatas ED, Jackson C, Roalf DR, Milham MP, Calkins ME, Hakonarson H, Gur RC, Gur RE (2015) Connectome-wide network analysis of youth with Psychosis-Spectrum symptoms. Mol Psychiatry 20:1508-1515.
Savla GN, Vella L, Armstrong CC, Penn DL, Twamley EW (2013) Deficits in domains of social cognition in schizophrenia: a meta-analysis of the empirical evidence. Schizophrenia bulletin 39:979-992.
Scheperjans F, Eickhoff SB, Homke L, Mohlberg H, Hermann K, Amunts K, Zilles K (2008) Probabilistic maps, morphometry, and variability of cytoarchitectonic areas in the human superior parietal cortex. Cereb Cortex 18:2141-2157.
Sergi MJ, Rassovsky Y, Widmark C, Reist C, Erhart S, Braff DL, Marder SR, Green MF (2007) Social cognition in schizophrenia: relationships with neurocognition and negative symptoms. Schizophr Res 90:316-324.
Shanmugan S, Wolf DH, Calkins ME, Moore TM, Ruparel K, Hopson RD, Vandekar SN, Roalf DR, Elliott MA, Jackson C, Gennatas ED, Leibenluft E, Pine DS, Shinohara RT, Hakonarson H, Gur RC, Gur RE, Satterthwaite TD (2016) Common and Dissociable Mechanisms of Executive System Dysfunction Across Psychiatric Disorders in Youth. Am J Psychiatry 173:517-526.
Sharma A, Wolf DH, Ciric R, Kable JW, Moore TM, Vandekar SN, Katchmar N, Daldal A, Ruparel K, Davatzikos C, Elliott MA, Calkins ME, Shinohara RT, Bassett DS, Satterthwaite TD (2017) Common Dimensional Reward Deficits

Across Mood and Psychotic Disorders: A Connectome-Wide Association Study. Am J Psychiatry:appiajp201616070774.
Shehzad Z, Kelly C, Reiss PT, Cameron Craddock R, Emerson JW, McMahon K, Copland DA, Castellanos FX, Milham MP (2014) A multivariate distance-based analytic framework for connectome-wide association studies. Neuroimage 93 Pt 1:74-94.
Sprong M, Schothorst P, Vos E, Hox J, van Engeland H (2007) Theory of mind in schizophrenia: meta-analysis. Br J Psychiatry 191:5-13.
van der Meer L, Groenewold NA, Pijnenborg M, Aleman A (2013) Psychosis-proneness and neural correlates of self-inhibition in theory of mind. PLoS One 8:e67774.
Van Essen DC, Drury HA, Dickson J, Harwell J, Hanlon D, Anderson CH (2001) An integrated software suite for surface-based analyses of cerebral cortex. J Am Med Inform Assoc 8:443-459.
Wang D, Buckner RL, Fox MD, Holt DJ, Holmes AJ, Stoecklein S, Langs G, Pan R, Qian T, Li K, Baker JT, Stufflebeam SM, Wang K, Wang X, Hong B, Liu H (2015a) Parcellating cortical functional networks in individuals. Nat Neurosci 18:1853-1860.
Wang J, Yang Y, Fan L, Xu J, Li C, Liu Y, Fox PT, Eickhoff SB, Yu C, Jiang T (2015b) Convergent functional architecture of the superior parietal lobule unraveled with multimodal neuroimaging approaches. Hum Brain Mapp 36:238-257.
Yan CG, Wang XD, Zuo XN, Zang YF (2016) DPABI: Data Processing & Analysis for (Resting-State) Brain Imaging. Neuroinformatics 14:339-351.
Yang GJ, Murray JD, Wang XJ, Glahn DC, Pearlson GD, Repovs G, Krystal JH, Anticevic A (2016) Functional hierarchy underlies preferential connectivity disturbances in schizophrenia. Proc Natl Acad Sci U S A 113:E219-228.